water

MDPI

Article

Wave Hindcast in Enclosed Basins: Comparison among SWAN, STWAVE and CMS-Wave Models

Chiara Favaretto [1,*], Luca Martinelli [1,2], Emma M. Philippine Vigneron [3] and Piero Ruol [1]

[1] ICEA Department, Padua University, v. Ognissanti 39, 35129 Padova, Italy; luca.martinelli@unipd.it (L.M.); piero.ruol@unipd.it (P.R.)
[2] Centro Giorgio Levi Cases, Padua University, v. Marzolo 9, 35131 Padova, Italy
[3] Independent Researcher, 13600 Ceyreste, France; emma.vigneron26@gmail.com
* Correspondence: chiara.favaretto.1@unipd.it

Abstract: This paper highlights the issue of the model consistency for wave hindcasts in enclosed basins, such as lakes and lagoons. For these applications, the wind input mechanism is essential and the differences in the model approaches and available settings make it critical and difficult for the users to comprehensively understand each of the model's capabilities and limitations. Therefore, three freely accessible regional scale spectral wave models (SWAN, STWAVE, and CMS-Wave), using the Half and Full plane modes where available, are used for wave hindcast purposes in two locations of the Garda Lake (IT). Results achieved with default settings are compared and discussed. Significant differences are found showing that, unfortunately, specific calibration, which is, however, not possible in many practical cases, is essential for applications in enclosed basins.

Keywords: wave generation; numerical models; SWAN; STWAVE; CMS-Wave; Garda Lake

Citation: Favaretto, C.; Martinelli, L.; Vigneron, E.M.P.; Ruol, P. Wave Hindcast in Enclosed Basins: Comparison among SWAN, STWAVE and CMS-Wave Models. *Water* **2022**, *14*, 1087. https://doi.org/10.3390/w14071087

Academic Editor: Diego Vicinanza

Received: 21 February 2022
Accepted: 25 March 2022
Published: 29 March 2022

1. Introduction

For small maritime and coastal projects, if the wave measurements are insufficiently characterized, it is nowadays a standard design practice to develop the wave statistic through numerical predictions based on available long-term wind data.

Wave models can be categorized based on their typical applications, i.e., global/oceanic or coastal/regional (Lavidas et al. [1], Umesh et al. [2]). Well-known ocean scale models are WAve Model (WAM, [3]) and WaveWatch 3 (WW3, Tolman, [4]), regional scale wave models are, among others, Simulating WAves Nearshore (SWAN, Booij et al. [5,6]), STeady-state spectral WAVE (STWAVE, Smith [7]), MIKE21-SW [8] and CMS-Wave (Lin at al. [9]). The models can be tuned through several settings and parameters. Actually, the experience on the best choice for settings and parameters is mainly site-specific and, in the absence of direct calibrations, the default values are suggested. A comprehensive discussion of the present state of the art in wave modelling and future developments is presented by Cavaleri et al. [10].

For small scale investigations, several works confirmed that the results are only partially affected by the actual model used. Rusu et al. [11] compared the predictions carried out with SWAN and STWAVE focusing on the performance of the two models in shallow and very shallow water, considering several target areas on the Portuguese coast. Fonseca et al. [12] used these results to compare also the MIKE 21 BW predictions. The authors found that the models behave similarly; MIKE 21 SW and SWAN are more complex models with a larger set of formulations and choices, but STWAVE, despite its simplicity, produced good results in a faster computational time. Strauss and al. [13] presented approximate results between SWAN and MIKE 21 SW for the Gold Coast in Australia; the SWAN model showed larger sensitivity to the wind input without results improvements. Ilia & O'Donnell [14] compared the results performed with SWAN and MIKE 21 SW on an unstructured grid representing a harbour in the presence of three

detached breakwaters. This study suggests the results of the models were consistent with observations during the storms and behaved similarly in most events. A sensitivity analysis demonstrates the wind effect was significant on the results due to the large fetch length in the harbour.

In practice, these papers demonstrated that the models simulate correctly the combined effect of wave propagation and wave generation mechanisms. For the specific case of enclosed basins, the wave generation is critical, since the wind-wave growth starts from land, the wave boundary condition being null. Nevertheless, although each model implements a different formulation for the wind input source term, and uses different relations for the drag coefficient, it is expected that the final result is similar. However, Moeini et al. [15], who investigated only the wind-wave generation (without a wave spectrum as boundary condition), found some inconsistency between the results of the SWAN and MIKE21 due to differences between the wind input parameterizations. Furthermore, different formulations are available also within the same model. Christakos et al. [16] and Aydoğan & Ayat [17] compared the different source term packages available in SWAN. They all perform well for the most exposed locations, but for more sheltered locations, the packages show pronounced differences.

Given the above literature review, it is evident that several studies have been carried out to compare different spectral wave models, but there is not sufficient focus on specific applications on enclosed basins, such as lakes and closed lagoons. The novelty of this research is the focus on these conditions for which it is interesting to examine whether the model's results are consistent.

In the present study, three freely accessible regional scale spectral wave models (SWAN, STWAVE, and CMS-Wave) are compared with reference to the wind-wave generation inside an enclosed basin. SWAN is widely applied by the scientific community for coastal and maritime studies (e.g., Bellotti et al. [18]). STWAVE is simpler in terms of formulations and settings and was already used by the Authors (Martinelli et al. [19], Favaretto et al. [20]). Finally, CMS-Wave is similar to STWAVE but with an emphasis on wave-structure-land interactions for practical coastal engineering projects (e.g., Nassar et al. [21]). Several studies discuss the validation of these three models with field data. For instance, Christakos et al. [16] studied the performance of three white-capping and wind input source term packages available in SWAN comparing the results with in situ measurements in a fjord system, i.e., a narrow fetch geometry. Bryant and Jensen [22] applied the STWAVE model to the North Atlantic coast modelling seven historical storm events (including hurricane Irene and Sandy). The STWAVE results were successfully compared against buoys measurements. The authors found a slightly smaller model performance within the Chesapeake Bay, a complex environment where waves are largely locally generated by winds. Lin et al. [23] verified and validated the CMS-Wave model with several test cases, including analytical/empirical solutions, idealized applications, and studies with data from laboratory and field measurements in coastal inlets, coastal structures, bays, estuaries, etc. The behavior of the models in the case of enclosed basins is not specifically documented.

Although for many applications, the absence of reliable simultaneous wind and wave information prevents a direct assessment of the model's performance, it is possible to point out the potential inaccuracy of the models based on their mutual comparison. In order to compare the performance of SWAN, STWAVE, and CMS-Wave, this study investigates an idealized case and a real application on the Garda Lake, in the North of Italy.

The objective of this study is to make the users more aware of the limits and peculiarities of these models applied to enclosed basins. Hence, the main default settings and parameters recommended by the model's developers are used, which are those reasonably chosen by most engineers in the frequent case of absence of specific calibrations (such as for the Garda Lake where, although many structures have been built, no calibration has ever been done).

Section 2 briefly describes the main characteristics of the three chosen models and the wind input source terms. In Section 3, an idealized case is presented to highlight the

differences in wind-wave generation and growth. Section 4 presents an application to the Garda Lake (Italy) and a comparison of the results carried out with the three wave spectral models. Finally, conclusions are drawn.

2. Numerical Models

SWAN, STWAVE, and CMS-Wave are spectral models based on the wave action balance equation. The models are available for free and can be run as a stand-alone executable. In the following brief descriptions of the models are presented; for a more detailed description of hypothesis and formulations, the readers can refer to the user and technical manuals.

The SWAN (Simulating WAves Nearshore) model is a third-generation wave model, developed by the Delft University of Technology (Booij et al. [5,6]). The model solves the wave action balance equation with sources and sinks and accounts for refraction, diffraction, shoaling, blocking and reflections by opposing currents, blocking, and reflection by or transmission through obstacles. The model can perform stationary and non-stationary simulations over structured or unstructured meshes. It solves the equations with a finite difference approach using an implicit iterative direct method for time integration (Sartini et al. [24]). The sources and sinks included are generation by wind, dissipation by whitecapping, dissipation by wave-breaking induced by depth, dissipation by bottom friction, wave-wave interactions in both deep and shallow water.

The STWAVE (STeady-state spectral WAVE) was developed by the U.S. Army Corps of Engineers Waterways Experiment Station (USACE-WES). STWAVE is a steady-state, finite difference, phase-averaged, spectral model based on the wave action balance equation, that can simulate nearshore wave propagation and transformation, including refraction, shoaling, breaking, and wind-wave generation (Smith, [7]).

The model has two modes of operation: half-plane and full-plane. Half-plane mode allows wave energy to propagate only from the offshore towards the nearshore. Hence, waves travelling in the negative x-direction, possibly due to reflection or winds, are neglected in half-plane simulations. The full-plane mode, instead, allows wave transformation and generation on the full 360-deg plane. The half-plane version requires considerably lower memory requirements, executes faster, and is generally appropriate for most nearshore coastal applications except for semi-enclosed bays and lakes where there is no obvious offshore direction. In these latter cases, the full-plane version is preferable.

CMS-Wave is a spectral wave transformation model (Lin et al. [9]) developed by the Coastal Inlets Research Program (CIRP), a research and development program of the U.S. Army Corps of Engineers (USACE). The model solves the wave-action balance equation using a forward marching finite difference method. CMS-Wave includes physical processes such as wave shoaling, refraction, diffraction, reflection, wave-current interaction, wave breaking, wind-wave generation, white capping of waves. One of the peculiarities of the CMS-Wave model is that it takes into account the influence of coastal structures in terms of diffraction, reflection, transmission, run-up, and setup. As for the STWAVE model, the CMS-Wave can be run both in Half and Full mode.

SWAN is a more flexible model that allows setting many parameters of the formulations for the source terms. STWAVE and CMS-Wave only allow to choose if including or not some phenomena. Both SWAN and CMS-Wave can perform stationary and non-stationary simulations, conversely, STWAVE runs only stationary simulations.

The STWAVE and the CMS-Wave models take advantage of the SMS interface (Zundel [25]) for grid generation, model setup and input, plotting, and post-processing of modelling results. To perform the simulations, the SMS 12.2.7 (for STWAVE and CMS-Wave) and the SWAN 41.31 are used.

2.1. Wind Input Source Terms

In the SWAN model, four options are available for third-generation mode for wind input, quadruplet interactions, and whitecapping: KOMEN, JANSSEN, WESTH, and ST6. They are described in detail in Christakos et al. [16] and Aydoğan & Ayat [17].

In the KOMEN and JANSEN packages, the transfer of wind energy to the waves is described by a resonance mechanism and a feedback mechanism, that have respectively linear and exponential effects (Equation (1)). If the linear growth (A) is activated, the expression proposed by Cavaleri & Malanotte-Rizzoli [26] is used (Equation (2)).

$$S_{in} = A + BE(\sigma, \theta) \tag{1}$$

$$A = \frac{1.5 \times 10^{-3}}{2\pi g^2}(u^* \max[0, \cos(\theta - \theta_w)])^4 H\,, \quad H = exp\left\{-\left(\frac{\sigma}{\sigma^*_{PM}}\right)^{-4}\right\} \tag{2}$$

In which θ_w is the wind direction, H is the filter and σ^*_{PM} is the peak frequency of the fully developed sea state ($\sigma^*_{PM} = 2\pi 0.13g/28\ u^*$).

The exponential effect of the wind input term in the KOMEN package is estimated according to Komen et al. [27]. The expression is a function of u^*/c_{ph}, where c_{ph} is the phase speed.

$$B = \max\left[0, 0.25\frac{\rho_a}{\rho_w}\left(28\frac{u^*}{c_{ph}}\right)\cos(\theta - \theta_w) - 1\right]\sigma \tag{3}$$

where ρ_a and ρ_w are the density of air and water, θ and θ_w the wave and wind direction.

In the JANSEN package, the exponential growth is described by the expression proposed by Janssen [28]. The WESTH package includes a non-linear saturation-based whitecapping combined with wind input of Yan [29], which combines the expressions by Komen et al. [27] and Plant [30].

Finally, the novel ST6 package uses the wind input and the whitecapping formulation from Rogers et al. [31]. This package is an observation-based scheme that contains wave-turbulence interaction, positive and negative wind input, and two-phase whitecapping dissipation. The wind input is described by:

$$S_{in}(\sigma, \theta) = \frac{\rho_a}{\rho_w}\sigma\left\{2.8 - [1 + \tanh\left(10\sqrt{B_n}W - 11\right)\right\}\sqrt{B_n}WE(\sigma, \theta) \tag{4}$$

where B_n is the spectral saturation.

Christakos et al. [16] found the best agreement with measurements for the KOMEN package for sheltered areas, and WESTH and ST6 for more exposed ones. Aydoğan & Ayat [17] found that ST6 physics presented the best model performance at predicting the wave heights for locations along the Black Sea coastline, which is an enclosed basin, but very large. The ST6 package requires specific calibration, including a coefficient that accounts for the effect of gustiness in the growth rate (raised from 28 to 32).

The wind velocity used by SWAN is the wind velocity at a 10 m elevation (U_{10}), then converted in the calculations into the friction velocity u^*, defined as $u^{*2} = C_D\ U_{10}{}^2$, where C_D is the wind-drag coefficient. In the following simulations, the default KOMEN package is used with the Wu [32] default formulation (Equation (5)) for the drag coefficient C_D. The 2nd order polynomial formula proposed by Zijlema et al. [33] (Equation (6)) and the Hwang [34] formulation (Equation (7)), default for the ST6 packages) are also tested for comparison, being choices typically used by designers.

$$C_{D\_Wu} = \begin{cases} 1.2875 \times 10^{-3} & \text{for } U_{10} < 7.5 \text{ m/s} \\ 10^{-3}(0.065U_{10} + 0.8) & \text{for } U_{10} \geq 7.5 \text{ m/s} \end{cases} \tag{5}$$

$$C_{D\_Zijlema} = 10^{-3}\left[-1.49\left(\frac{U_{10}}{31.5}\right)^2 + 2.97\left(\frac{U_{10}}{31.5}\right) + 0.55\right] \tag{6}$$

$$C_{D\_Hwang} = 10^{-4}\left(-0.016{U_{10}}^2 + 0.967U_{10} + 8.058\right) \quad (7)$$

The flux of energy due to the wind source is implemented into STWAVE by the equation proposed by Resio [35]:

$$F_{in} = 0.85\lambda \frac{\rho_a}{\rho_w} C_m \frac{u^{*2}}{g} \quad (8)$$

The friction velocity u^*, defined as before $u^{*2} = C_D\ {U_{10}}^2$, is computed through the drag coefficient $C_D = 0.0012 + 0.000025\ U_{10}$. C_m is the mean wave celerity, ρ_a and ρ_w are the density of air and water, and λ is a partitioning coefficient that represents the percentage of total atmosphere to water momentum transfer that goes directly to the wave field (usually $\lambda = 0.75$).

The wind-input source in the CMS-Wave model is formulated as a function of the ratio of wave celerity C to wind speed W, the ratio of wave group velocity Cg to wind speed, the difference of wind speed and wave celerity, and the difference between wind direction θ_{wind} and wave direction θ (Lin & Lin [36]):

$$S_{in} = \frac{a_1\sigma}{g} F_1\left(\vec{W} - \vec{Cg}\right) F_2\left(\frac{Cg}{W}\right) {E^*}_{PM}(\sigma)\Phi(\theta) + \frac{a_1\sigma^2}{g} F_1\left(\vec{W} - \vec{Cg}\right) F_2\left(\frac{Cg}{W}\right) F_3\left(\frac{Cg}{W}\right) N \quad (9)$$

where N is the wave action density ($=E(\theta,\sigma)/\sigma$), ${E^*}_{PM}$ is the functional form of the Pierson-Moskowitz spectrum, $\sigma = g/W$ is the Phillips constant, and $\Phi(\theta)$ is a normalized directional spreading. The function F_1 describes the wind stress effect, F_2 designates Phillips' mechanisms (Phillips [37]), and F_3 accounts for the wave age effect.

2.2. Models Parameters and Settings

In the following simulations, the SWAN model is run with the third generation option (GEN3) in stationary mode. Default numerical properties are used with NUMerics STOPC command (*dabs* = 0.005, *drel* = 0.01, *curvat* = 0.005, *npnts* = 99.5) with limiter parameter equal to 0.1. This command influences the convergence criterion for terminating the iterative procedure in the computations [38]. The threshold depth *depmin* is set equal to 0.05 m, as default, indicating that any positive depth smaller than *depmin* is made equal to this value.

For the depth-induced wave breaking, the default Battjes and Janssen [39] formulation is used (BREA command) with *alpha* = 1 and *gamma* = 0.73. The bottom friction is activated with the FRIC MAD command that considers the eddy-viscosity model of Madsen et al. [40]. The equivalent roughness length scale of the bottom *kn* is set as default (0.05 m), and following the Bretschneider et al. [41] relationship, it corresponds to a Manning coefficient of 0.04 $s/m^{1/3}$ in shallow water.

To consider the Zijlema et al. [33] formulation, the DRAG FIT command is used. To activate the ST6 package the GEN3 ST6 command is employed. Since there is no default ST6 parameter set available, one of the example parameter sets given in [42] was used. The selected ST6 parametrization considers *a1sds*, *a2sds*, *p1sds*, *p2sds*, and *wscaling* parameters equal to 2.8×10^{-6}, 3.5×10^{-5}, 4, 4, and 32 respectively. Aydoğan & Ayat [17] found that this latter parameter is the most significant in the ST6 package at adjusting wave heights. The ST6 package requires also the setting of the type of swell dissipation and, as suggested by the example, the non-breaking dissipation of Ardhuin et al. [43] is used with *cdsv* = 1.2.

For the STWAVE and the CMS-Wave models, the lists of available adjustable parameters are shorter than the SWAN one. In the STWAVE model the depth type is set as *non-transient* and the boundary interpolation as *morphic*. Current interaction is not considered, the bottom friction is spatially constant, and the Manning coefficient is $n = 0.04\ s/m^{1/3}$. Default iteration control options are used: maximum number of initial and final iterations = 20; initial and final iterations stop values = 0.1; initial iterations stop percent = 100 and final iterations stop percent = 99.8.

In the CMS-Wave model, the bottom friction is set constant with $n = 0.04\ s/m^{1/3}$, and the "wetting and drying" option is allowed. The infragravity wave effect and the non-linear wave effect are activated, and the diffraction intensity is set equal to 4 as default. The wave breaking formulation employed is the "extended Goda" option (Sakai et al. [44]).

3. Comparison Based on an Idealized Basin Test

The purpose of this section is to compare the wave generation and wave growth prediction of the three models in an idealized basin, minimizing the effects of diffraction, refraction, shoaling, and reflection. The model domain is a square basin (20 km × 20 km) consisting of 100 × 100 cells with constant size (200 m × 200 m). A preliminary investigation showed that no significant changes are observed for a grid size of 100 m, 200 m, and 400 m, and we concluded that 200 m was the best compromise between speed and accuracy. The bottom is flat and constant, and the simulations were performed two times, in the first considering a water depth d = 20 m and in the second d = 100 m. Bed friction is not taken into account. The test cases include 14 constant winds, ranging from 5 m/s to 50 m/s with wind direction along one of the two axes of the grid. The wave energy input at the upwind boundary is set to zero.

The spectral grid used in the three models ranges from 0.12 to 1 Hz, but different numbers of frequency bins are set. In fact, this is a crucial and critical issue for the numerical models since it should be a compromise between accuracy and computational load. The frequency range must cover the range of expected wave frequencies generated by the winds, and can be approximately found using well known analytical formulations (e.g., [45,46]) based on intensity, fetch, duration and depth. The setting of an unsuited frequency range and discretization lead to noteworthy results (with differences of the order of 50–60% for the wave height). For the SWAN model, the number of bins is 60, and the model chooses the intervals as logarithmically distributed. For the STWAVE model, the number of bins is 111 and regularly distributed with a 0.008 Hz increment. Finally, for the CMS-Wave model, the number of bins is 74 with a 0.012 Hz increment. The other settings and parameters for all the models are set to the default choices and values. The directional distribution of the energy is discretized with a 5° interval.

The results are evaluated at the centre line of the basin, where the boundary effects are negligible, every 1 km of fetch. Figure 1 shows the model domain, the output locations, and an example of results carried out with the STWAVE model in Full mode, for a wind intensity equal to 25 m/s. In the Northern boundary, the wave height is zero since the condition is a non-reflective beach, that, however, does not affect the result in the domain.

The STWAVE model and the CMS-Wave model are run in both Half and Full mode. For this particular idealized basin, where the main geometrical wave transformation phenomena are negligible due to the basin configuration, the results in the centre line performed in Half and Full mode for both models are comparable (with differences of the order of ±2–7% both for *Hs* and *Tp*). In the following, some results are presented only for the Full mode setting.

This test case is also suited to be compared with the wave growth curves proposed by Hurdle and Stive [45], which are a modification of the ones given in the Shore Protection Manual (SPM, 1984 [46]).

Figure 2 shows the comparison among the results for the idealized test case with wind intensity equal to 20 m/s in terms of wave heights and wave periods as a function of the fetch. The figures show both the analytical results carried out with the SPM (1984, [46]) formula and the Hurdle and Stive formula and the numerical results performed with STWAVE (Half and Full mode), CMS-Wave (Half and Full mode), and SWAN. As aforementioned, the differences between the Half and Full mode for STWAVE and CMS-Wave are small (green/red lines and star markers are similar between them). The three models behave differently, and this is interpreted as a consequence of the different formulations of the wind input and wave growth implemented in the codes. The figures are essentially a proxy for the mechanism that transfers energy from the wind with constant velocity to the waves.

The figures also show that CMS-Wave has some issues in the modelling of the waves for fetches smaller than 5 km.

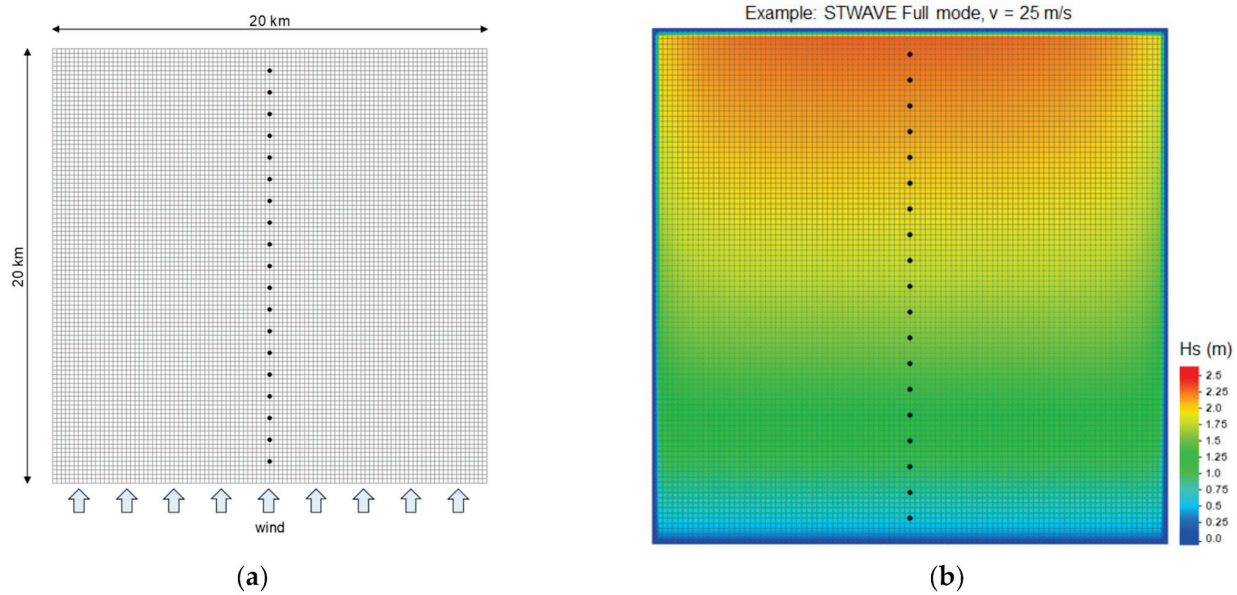

Figure 1. Idealized test basin: (**a**) model domain and output locations, i.e., black points in the centre line (**b**) example of results for the simulations carried out with the STWAVE model (Full mode) for a wind intensity equal to 25 m/s.

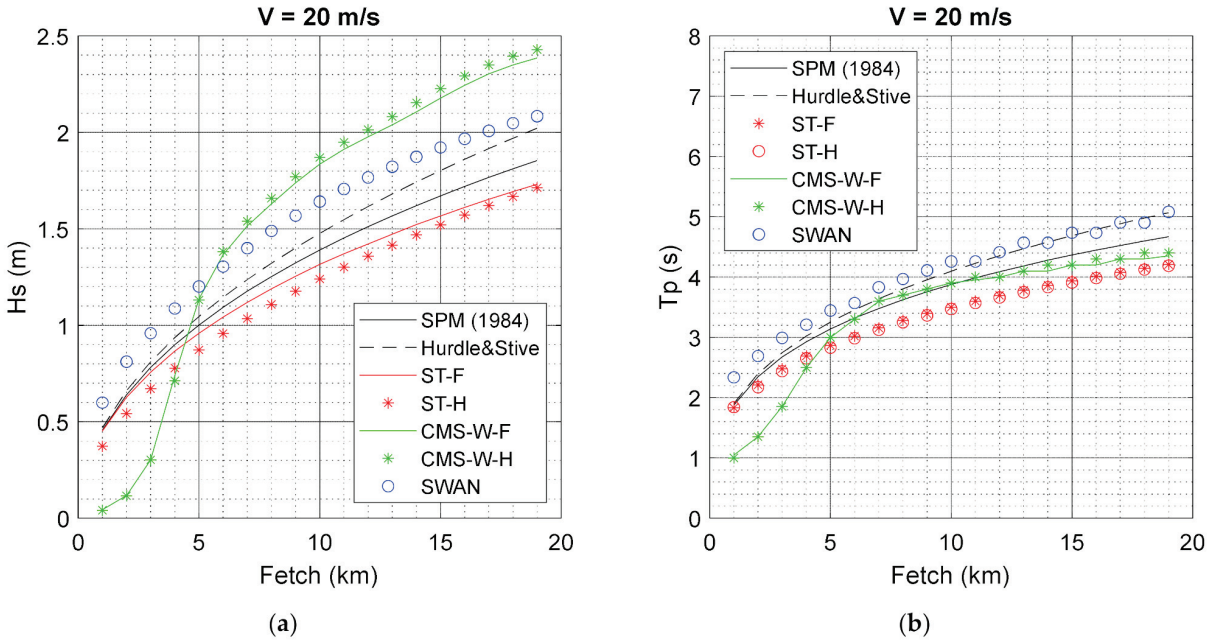

Figure 2. Comparison of the results for the idealized test case with wind intensity equal to 20 m/s, (**a**) wave heights as a function of the fetch; (**b**) wave periods as a function of the fetch. The figures show the analytical results carried out with the SPM (1984) formula and the Hurdle and Stive formula and the numerical results performed with STWAVE (Half and Full mode), CMS-Wave (Half and Full mode) and SWAN.

Nekouee et al. [47] carried out a similar idealized investigation through an extensive set of SWAN simulations for different lake geometries and wind conditions, using different

computational grid sizes to study the wave regime in order to compare numerical and empirical wave prediction methods. The authors find, with reference to the SWAN model, similar differences between the prediction and the analytical solution. Specifically, they found that CEM (Coastal Engineering Manual, [48]) analytical method shows more coincidence with the SWAN numerical wave prediction results in shallow lakes while SPM [46] and Krylov methods ([49]) agree better with SWAN results in deep water.

Figure 3 shows the evolution of the wave spectra in the three models. The SWAN spectra reflect the input source exponential shape and the non-linear wave interaction with energy transfer from higher to lower frequencies. The complicated input function (Equations (1)–(3)) for SWAN is reflected into a slightly more irregular shape of the spectrum compared to STWAVE, which shows a similar non-linear interaction behavior although with lower magnitudes. CMS-Wave suffers from a lower frequency resolution (which cannot be increased) and limited input energy at frequencies larger than 0.45 Hz (recall that the chosen frequency range is 0.12–1 Hz divided into 74 equally spaced bins). This explains why, for small fetches, the wave is not well generated.

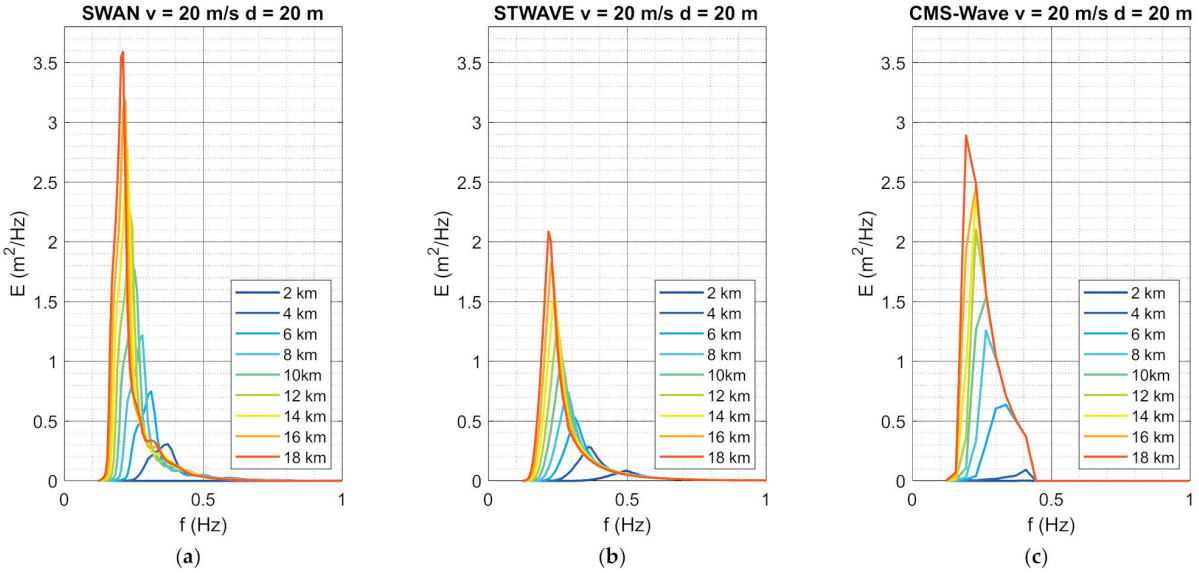

Figure 3. Evolution of wave spectra for the idealized test case with wind intensity equal to 20 m/s and depth equal to 20 m. (**a**) SWAN model; (**b**) STWAVE model and (**c**) CMS-Wave model.

To assess the comparison of the estimates with the results gathered with the analytical formula, three performance metrics are calculated: the coefficient of efficiency *NSE* Nash et al. [50], the index of agreement *D* Willmott et al. [51] and the square of the determination coefficient r^2. Complete disagreement is described by $D = 0$, $r^2 = 0$ and negative *NSE*. All indexed are = 1 for perfect agreement.

Table 1 summarizes the performance indexes between the models' results and the analytical results based on the formula proposed by Hurdle and Stive. SWAN and STWAVE (Full mode) are in good agreement with the analytical predictions. The performance of the CMS-Wave model seems less good.

Table 1. Performance indexes between the models' results and the analytical results based on the formula for the wave growth proposed by Hurdle and Stive [38].

		d = 20 m			d = 100 m		
	Value	***NSE***	***D***	r^2	***NSE***	***D***	r^2
SWAN	*Hs*	0.9436	0.9831	0.9438	0.9514	0.9857	0.9515
	Tp	0.9723	0.9928	0.9723	0.9722	0.993	0.9722
STWAVE (Full mode)	*Hs*	0.9507	0.9856	0.9518	0.9523	0.986	0.9533
	Tp	0.8505	0.9568	0.8656	0.8619	0.9607	0.8751
CMS-Wave (Full mode)	*Hs*	0.8224	0.9472	0.8248	0.8335	0.9509	0.8354
	Tp	0.4726	0.8705	0.5039	0.5301	0.8859	0.5559

As aforementioned, the CMS-Wave results for very small fetches are not consistent with the analytical results. A similar test case was performed by Lin et al. [52] for the CMS-Wave model, with a thinner basin (2 km × 20 km), water depth of 20 m, and three wind velocities (10, 20, 30 m/s) blowing parallel to the longer axis. Their results show some differences of the order of 10% in the comparison with the SPM (1984) curves for fetch larger than 5 km. They considered this behavior reliable for wave generation and growth for coastal applications but suggested further verification with field measurements. In the present study, we concluded that CMS-Wave can be applied for wave generation and growth in the coastal and estuary area with fetches greater than 5 km.

The observed differences among the models reasonably depend on the different numerical schemes adopted and the different sources of wind inputs implemented. In fact, as seen in Section 2.1, the formulations that described the wave growth by wind are dissimilar and consider different drag coefficients, not easy to harmonize, and for which a direct comparison is therefore not practical. To better investigate these differences from a global perspective, Figure 4 shows the ratio between the value of *Hs* computed with SWAN and the *Hs* computed with the other models for the same wind. The geometry of the idealized case is designed to minimize the effects of the boundary conditions and therefore the differences in the results can be ascribed only to the specific wind formulations and implementations of the models.

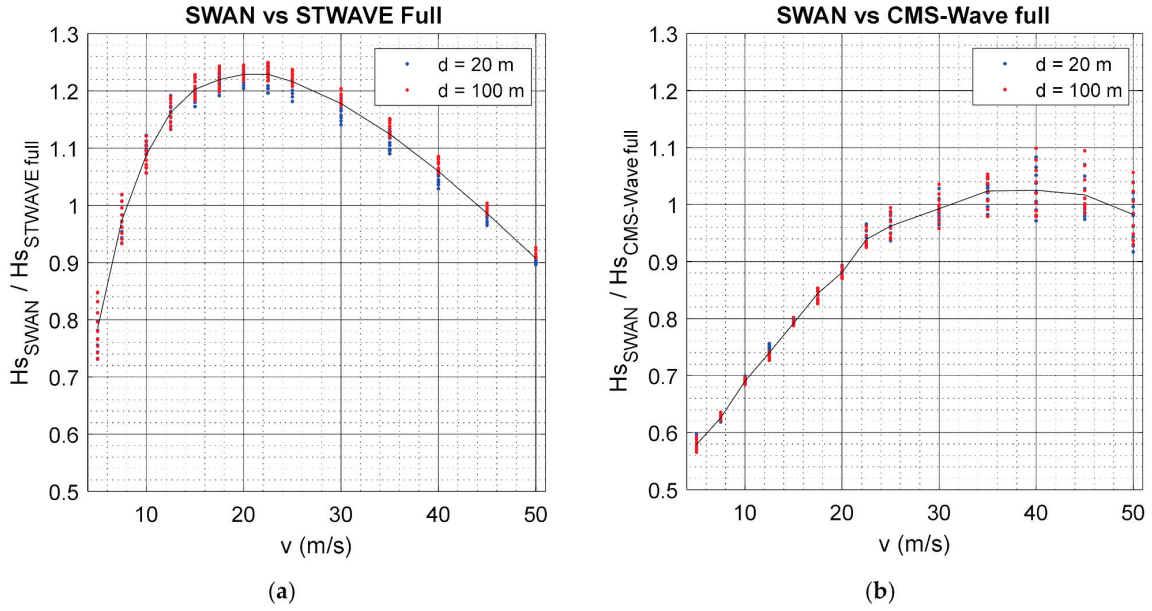

Figure 4. Ratio between the Hs results obtained with the SWAN model and the other models: (**a**) SWAN vs STWAVE, (**b**) SWAN vs CMS-Wave.

The different points, vertically aligned and with the same colour in the figure, are relative to the different fetch varying from 1 km to 19 km (output locations shown in Figure 1a). SWAN predicts waves higher (up to 25% higher) than STWAVE in the frequently investigated range of winds from 10 m/s to 40 m/s. Conversely, SWAN predicts waves smaller than CMS-Wave for winds lower than 30 m/s, and for higher winds the results carried out with the two models are comparable (differences of the order of 5%).

Accordingly to the differences among the predictions of the wave heights, also the wave periods are different. SWAN forecasts wave periods up to 20% larger than the other models for winds between 15–35 m/s.

Figures 5 and 6 show a comparison in terms of H_s and T_p evaluated at the centerline of the idealized case using different formulations of the wind drag available within SWAN. In fact, recent developments have suggested switching from the original formulation by Wu [32] to the formulation proposed by Zijlema et al. [33] or to the one proposed within the ST6 Package (Hwang [34]). As expected, since the tested wind velocities are not extreme, the two alternatives of the KOMEN package are very similar, whereas the ST6 package (using the settings recommended in regular SWAN simulations, with wind scaling equal to 32) shows lower values (25% lower) of wave height for more intense winds.

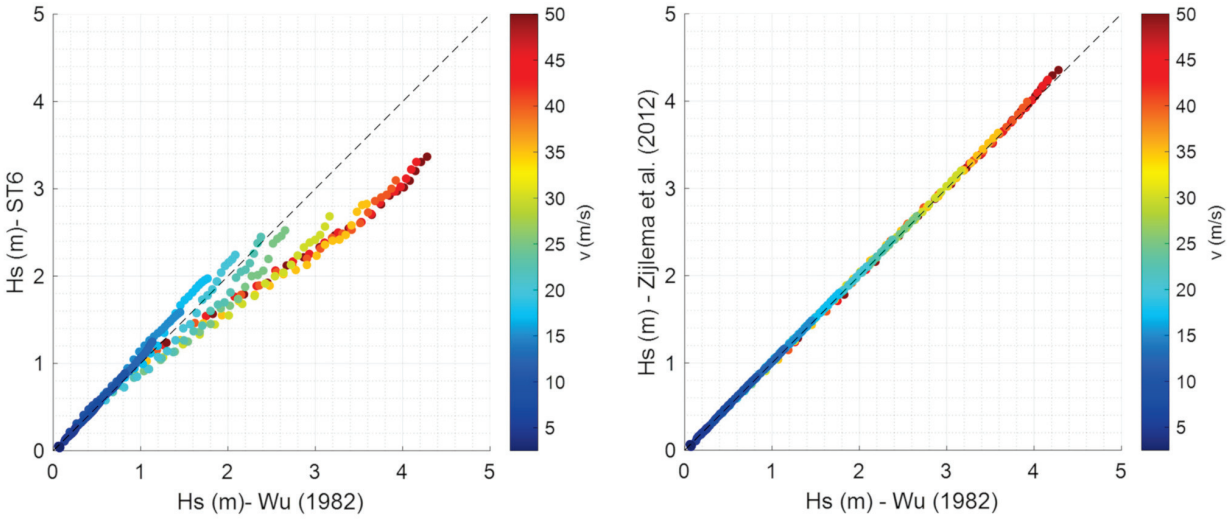

(**a**) (**b**)

Figure 5. Comparison in terms of H_s along the centerline of different formulations of the wind drag within (**a**) SWAN Package KOMEN (Wu [32] and Zijlema et al., [33]) and (**b**) SWAN Package ST6 (Hwang, [34]).

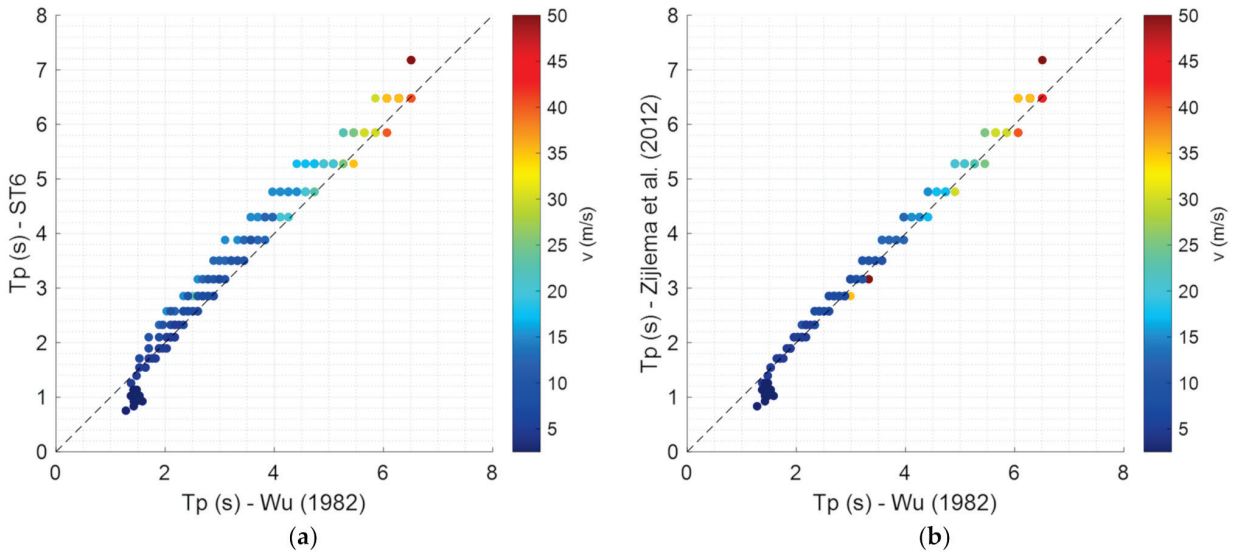

Figure 6. Comparison in terms of T_p along the centerline of different formulations of the wind drag within (**a**) SWAN Package KOMEN (Wu [32] and Zijlema et al., [33]) and (**b**) SWAN Package ST6 (Hwang, [34]).

4. Application to the Garda Lake (Italy)

4.1. Investigated Area

The investigated area is the Garda Lake, situated in the Italian alpine region, between Milan and Venice. It is the largest lake in Italy, with a surface area of 369.96 km^2 and a volume of 50.35 km^3. Its maximum length and maximum width are respectively 51.6 km and 16.7 km. The Garda Lake has an average depth of 136 m and a maximum depth of 346 m. Its surface is elevated on average at 65 m.a.s.l. but varies due to the regulation of the lake (Hinegk et al. [53]). The bathymetry of the lake is depicted in Figure 7, where the 0 level corresponds to a water level at 61 m.a.s.l.

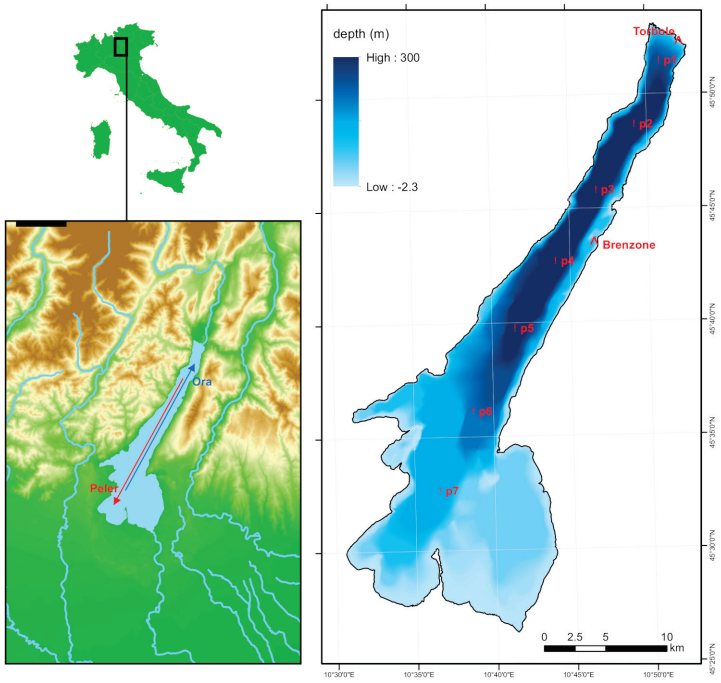

Figure 7. Investigated area, Garda Lake: location, main wind directions and bathymetry.

Winds correspond to movements of air due to differences in temperature and pressure between the two parts of Garda Lake (Giovannini et al. [54,55]). At North, the lake is surrounded by mountains while the Southern part is located in the Po River plain. This difference in meteorological conditions between the mountains and the plain creates the main winds on the Garda Lake: the Pelèr and the Ora, shown in Figure 7. The Pelèr wind blows from North to South, at a direction approximately equal to 30°. It starts at 2 a.m. and blows until noon. This wind is more intense on the Eastern side of the lake. The Ora wind blows from South to North, at direction opposite to the one of the Pelèr, approximately equal to 210°. It starts after the Pelèr stops from noon until sundown. It reaches its maximum intensity at North due to the narrowing of the lake creating a Venturi effect, and in this zone, it is responsible for high wave height.

A recent project for the construction of a bicycle lane (named "Ciclovia del Garda") around the Garda Lake requires extending the shoreline in some locations. An innovative method is employed, called the Sirive Barrier, adapted to the steep slope of the lake shores. The barrier was invented and built by Dalla Gassa s.r.l. (www.dallagassa.com, accessed on 1 March 2022) and it is a low-cost and environmentally friendly solution. The Sirive barrier consists of retaining plates used to support a rubble mound structure.

To design the barrier, the estimation of the wave characteristics related to a return period is essential. Unfortunately, waves are not measured in Garda Lake. The locations of interest are situated in Brenzone and Torbole (Figure 7). Brenzone is situated on the eastern coast of the lake, in the province of Verona, in the Veneto region. Torbole is situated in the Northern part of the lake, in the Province of Trento, in the Trentino Alto-Adige region. The winds in Torbole make it an attractive destination for sailing and windsurfing.

A statistical analysis was carried out on available wind datasets from several meteorological stations located in the western and northern sides of the lake. For both the locations a wind of 17 m/s coming from the Ora direction has a return period T_R of 10 years. Only these winds coming from the South generate waves in front of Torbole. For Brenzone, a wind of 15 m/s coming from the Peler direction has T_R = 10 years. Direct wind measurements are more reliable than simulated data since, where the surface winds are affected by the land's presence, the skill of wind models diminishes (de León and Soares, [56]).

4.2. Simulation Programme and Settings

A set of 30 simulations are performed to analyze the wind waves at the Garda Lake, with an initial water level taken equal to 0 m. The simulations are steady-state runs that consider a uniform wind field and a null wave spectrum at the upwind boundary, in order to evaluate only the wind-generated waves. The simulation programme includes 15 wind intensity V (2.5–50 m/s) and 2 wind directions D_W (Peler: 30° N and Ora: 210° N).

The grids used for the simulations are structured and regular with a resolution of 100 m. This spatial resolution is chosen in order to properly describe the details of the Garda Lake based on the available bathymetric dataset. The grid for SWAN is formed by 138,444 elements and is North-oriented. Conversely, the grids for the STWAVE and CMS-Wave models, formed by 109,931 elements, are oriented parallel to the simulated wind direction, as suggested by the developers.

The directional grid ranges from 0 to 360° N with 72 bins (interval = 5° N). The frequency grid is defined by a minimum frequency equal to 0.05 Hz, a maximum frequency equal to 2 Hz and the number of bins in the grid. As suggested by Bottema et al. [57], this upper value is required to properly resolve the spectrum and for hindcasting/forecasting waves in inland lakes. The frequency bins in SWAN are logarithmically distributed, conversely for the other two models the grid is homogenously subdivided. The number of bins is set to 36 for SWAN and 40 for STWAVE and CMS-Wave. These values were chosen to cover the entire spectra for the range of wind velocities used in the simulations.

A detailed discretization of the spectra requires a frequency step Δf sufficiently small to describe the peaks. For typical Jonswap spectra, with a period ranging from 1 s to 10 s,

the spectrum width is sufficiently well described with a Δf larger than, say, 0.05 Hz. This Δf covers the range of 0.05–2 Hz with 40 bins. The logarithmic scale used by SWAN requires a slightly smaller number of bins than the linear discretization used by STWAVE and CMS-Wave, and therefore we choose for the latter model 36 bins. A preliminary analysis showed that, in terms of results, the modelled wave height tends to converge when the Δf is consistent with this observation. This is shown for the SWAN model in Figure 8 which shows the ratio between the wave heights computed with n bins divided by the wave heights computed using 36 bins. The results are relative to the 7 points and the two nearshore locations (Figure 7), assuming wind velocity equal to 15 m/s and direction of 210° N. Further increasing the number of bins has only minor consequences, less than 1%, and an acceptable limit of the bin number is a value that must be larger than, say, 20.

The typical computational time for each run is of the order of 530–580 s for SWAN and STWAVE and of 290–350 s for CMS-Wave on an Intel Xeon E5-1650 v3 (3.50 GHz) computer equipped with 32 GB of RAM.

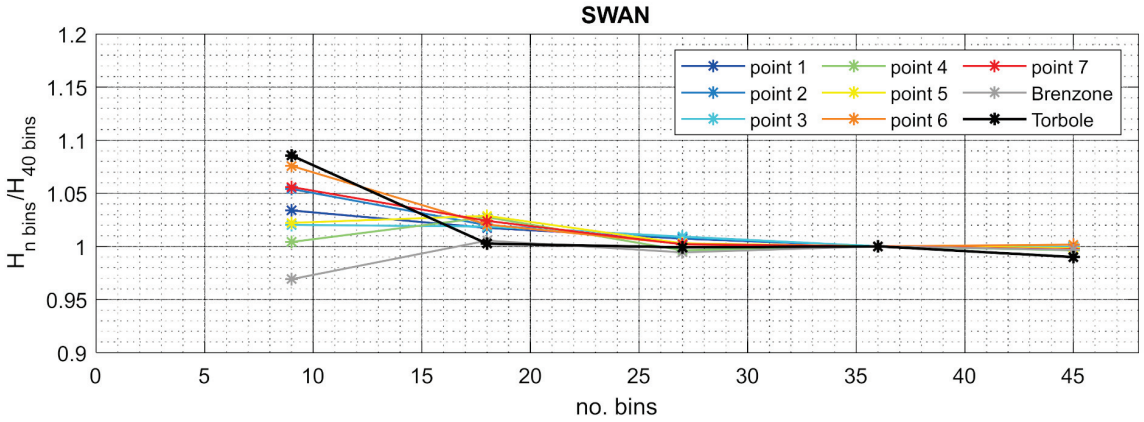

Figure 8. Ratio between the wave height computed with n bins divided by the wave height computed using 36 bins. The results are relative to the 7 points and the two nearshore locations, assuming wind velocity equal to 15 m/s and direction of 210° N.

4.3. STWAVE and CMS-Wave Models: Comparisons between Half and Full Mode

The behaviours of the STWAVE and CMS-Wave in the two available modes (Half and Full plane) cannot be overlooked since, for these simulations and conversely to the idealized basin, the wave transformations phenomena (such as the diffraction) are essential for the correct representation of the waves. The developers of the two models suggest using the Full mode in the case of an enclosed basin such as the Garda Lake.

For the STWAVE model, the main differences are in the shadowed areas, where the Half mode is not representative. Figure 9 shows the comparisons between wave heights predicted with the Half and Full mode for the STWAVE model. Panel (a) shows the comparison in the 7 points along the centre line of the Garda Lake and the Brenzone and Torbole locations (the locations are highlighted in Figure 7). The main differences are in the two locations near the shore where the effect of diffraction is consistent. Panel (b) shows the comparison of the wave height computed in all the grid points for a wind of 25 m/s blowing from the Ora direction. The majority of the points stay on a 1:1 line, but the scatter is wide due to the improvements of the results for the Full mode near the shore.

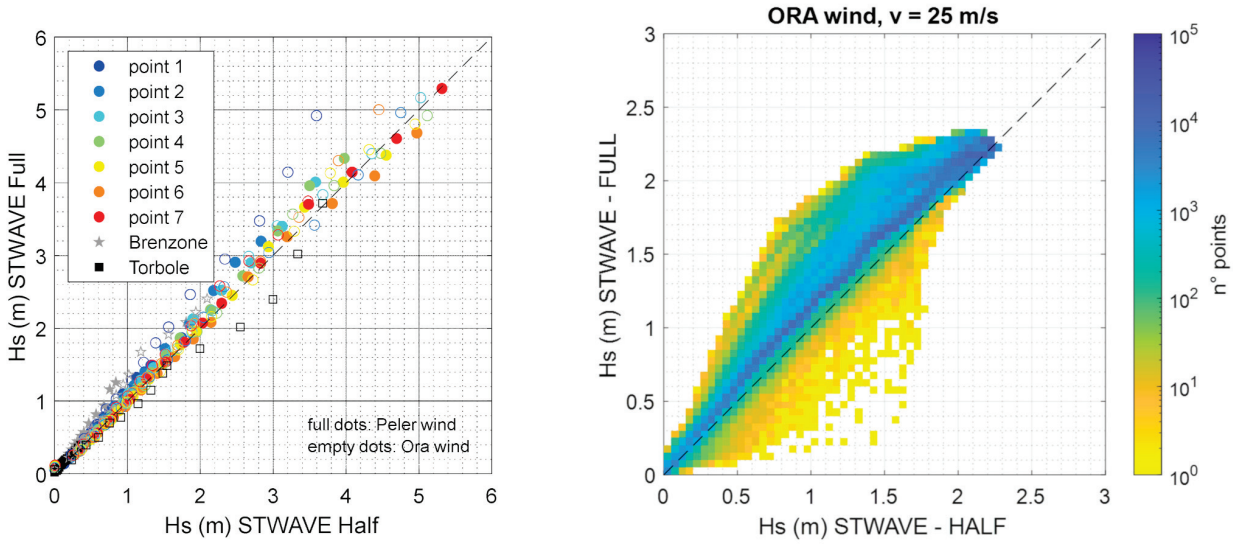

(**a**) (**b**)

Figure 9. Comparison between wave heights predicted with the Half and Full mode for the STWAVE model: (**a**) Comparison in the 7 points along the center line of the Garda lake and the Brenzone and Torbole locations; these locations are highlighted in Figure 7; (**b**) Comparison of the wave height computed in all the grid points for a wind of 25 m/s blowing from 210° N.

Figure 10 shows the same graphs computed with the Half and Full mode for the CMS-Wave model. For this model, the differences between the two modes are almost negligible.

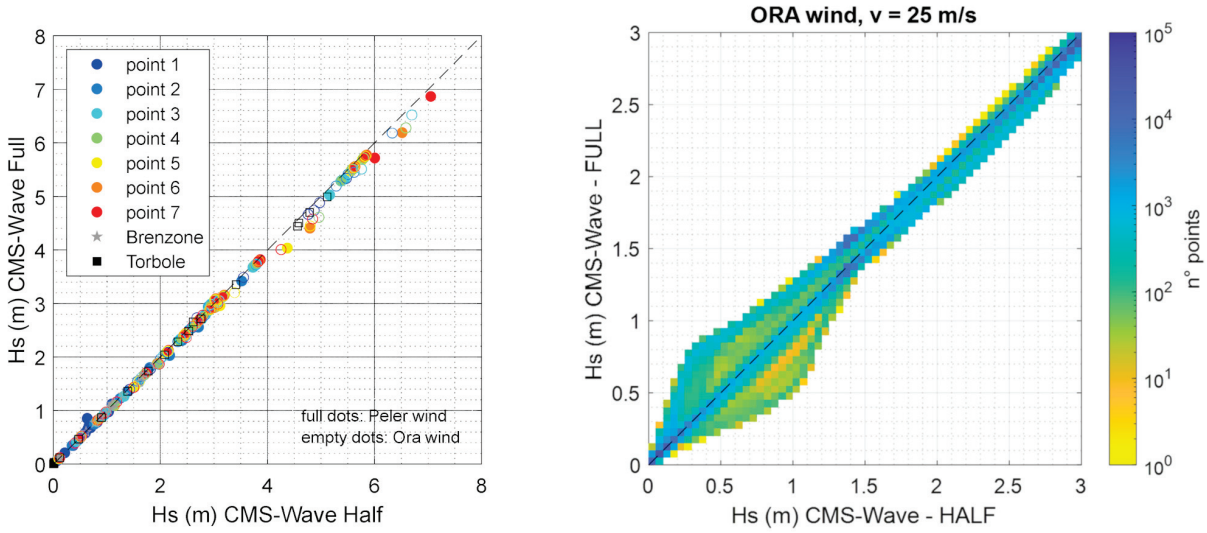

(**a**) (**b**)

Figure 10. Comparison between wave heights predicted with the Half and Full mode for the CMS-Wave model: (**a**) Comparison in the 7 points along the center line of the Garda lake and the Brenzone and Torbole locations; these locations are highlighted in Figure 7; (**b**) Comparison of the wave height computed in all the grid points for a wind of 25 m/s blowing from 210° N.

4.4. Comparisons among SWAN, STWAVE and CMS-Wave Models

Figures 11 and 12 show the comparison among the results carried out with the three models, for a wind intensity of 25 m/s blowing from direction 210° N (Ora) and 30° N (Peler). The origin of the maps has coordinates: LON 10.507311°, LAT 45.440319°, and the maps have the same colorbar limits.

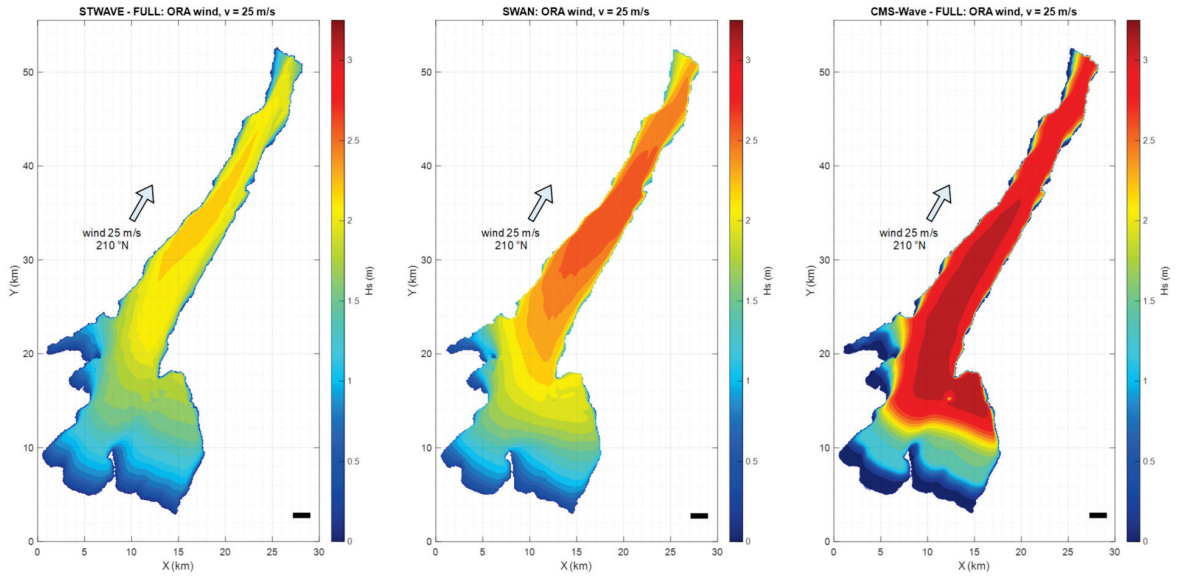

(**a**) (**b**) (**c**)

Figure 11. Wave heights for a wind intensity of 25 m/s blowing from direction 210° N (Ora wind) at the Garda Lake. (**a**) Results computed with the STWAVE model, Full mode. (**b**) Results computed with the SWAN model. (**c**) Results computed with the CMS-Wave model, Full mode.

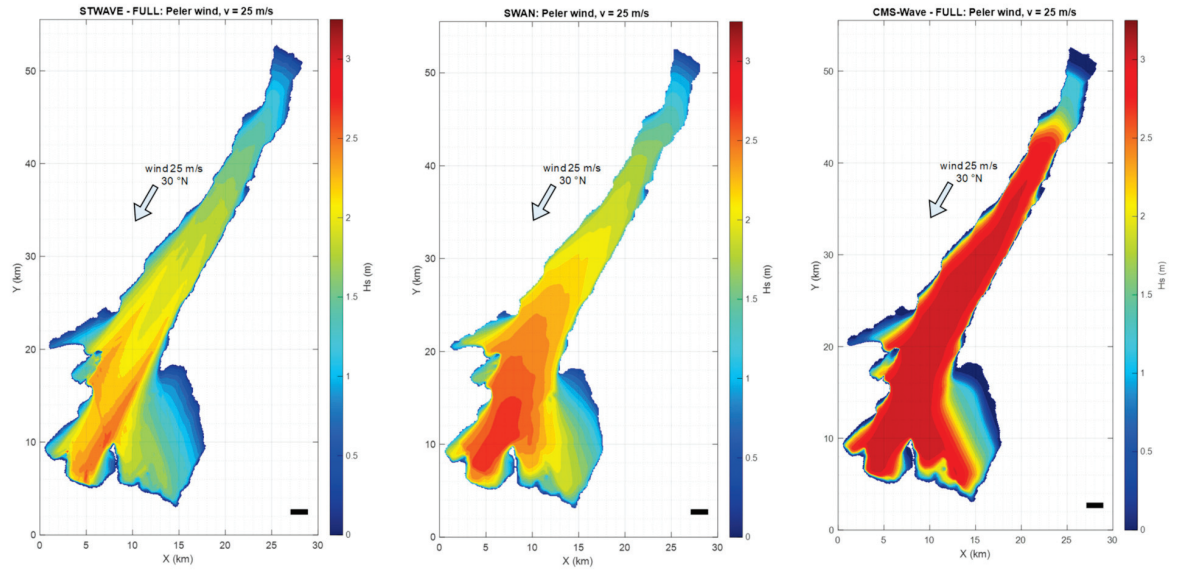

(**a**) (**b**) (**c**)

Figure 12. Wave heights for a wind intensity of 25 m/s blowing from direction 30° N (Peler wind) at the Garda Lake. (**a**) Results computed with the STWAVE model, Full mode. (**b**) Results computed with the SWAN model. (**c**) Results computed with the CMS-Wave model, Full mode.

SWAN and STWAVE show a similar pattern in terms of how the wave height is distributed along the lake, although the absolute value of the wave heights is 20–30% larger for the former model. CMS-Wave shows a different wave pattern with waves higher than the other two models (more than 100% in some locations). Moreover, the wave generation area that is comprised below 5 km of fetch is not representative as mentioned before.

Figure 13 shows the results for winds ranging from 2.5 to 25 m/s for the two tested wind directions carried out with the three models and the Hurdle and Stive formula and

evaluated at the two locations of interest (Torbole and Brenzone). To evaluate the analytical results, the depth is set equal to 130 m and the effective fetch F_E are:

- Brenzone: F_E = 1.76 km for the Peler direction, F_E = 7.62 km for the Ora direction.
- Torbole: F_E = 0.2 km for the Peler direction, F_E = 9.07 km for the Ora direction.

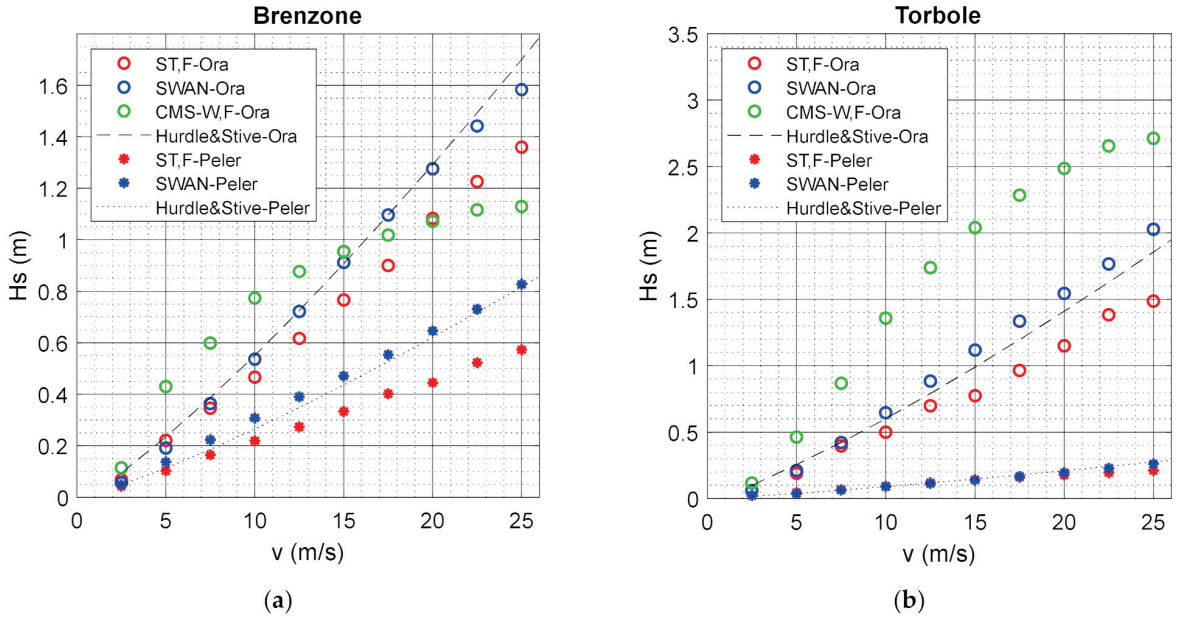

Figure 13. Comparison of the results for winds ranging from 2.5 m/s to 25 m/s blowing from 210° N and 30° N; (**a**) Brenzone (**b**) Torbole. The figures show the analytical results carried out with the Hurdle and Stive formula and the numerical results performed with STWAVE (Full mode), CMS-Wave (Full mode) and SWAN.

The results obtained with higher wind intensities are not included since they are not useful for design purposes. Hence, for the Peler wind, the results of CMS-Wave are not presented since both the locations, for this specific wind direction, have a fetch smaller than 5 km. For the two locations of interest, SWAN and STWAVE follow the simplified result proposed by the Hurdle and Stive formula, although the latter is constantly slightly smaller. CMS-Wave shows a different trend.

In order to better understand the effect of the wave propagation, a tentative harmonization of the wind input among the three models was carried out. In practice, it is assumed that the effect of the different formulations used for the wind-wave generation and growth (also including the different drag coefficients) found for the idealized case are generally valid. Therefore, the results obtained with the STWAVE and CMS-Wave models (in Full mode) and evaluated in the 7 points (shown in Figure 7) and in the two locations of interest are corrected with the ratio presented in Figure 4. The results of such correction are shown in Figure 14 together with the original results. The corrected STWAVE results are in good agreement with the values predicted by SWAN, both for the points in the centerline and at the location of interest, showing that the wave propagation is consistent among these models and different from the third one.

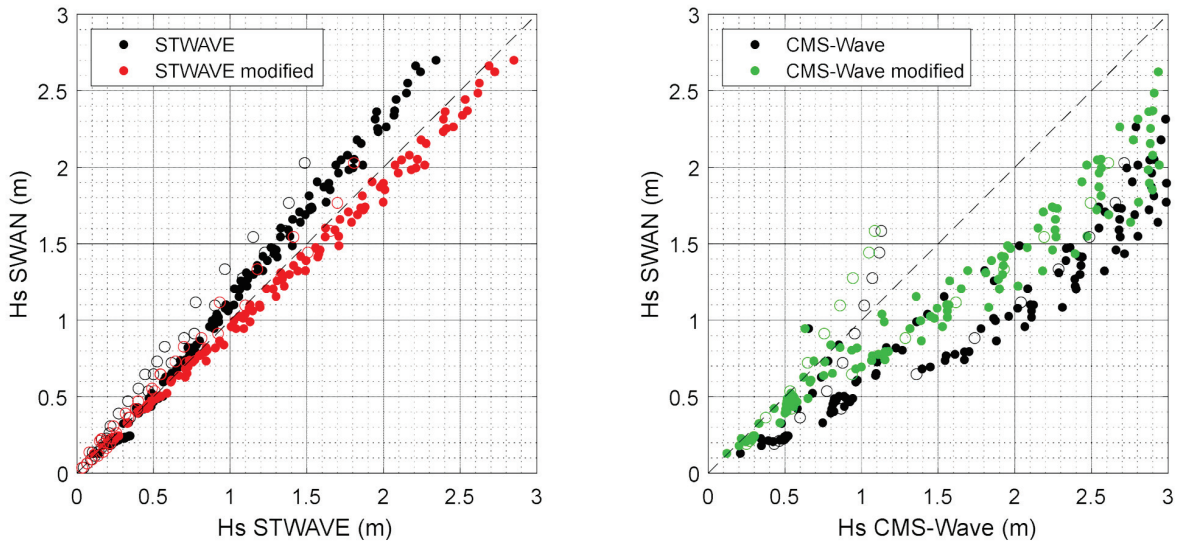

(**a**) (**b**)

Figure 14. Comparisons of the results evaluated in the 7 points (full dots) shown in Figure 7 and in the two locations of interest Brenzone and Torbole (empty dots): (**a**) STWAVE results plotted against SWAN results, including also the correction shown in Figure 4a; (**b**) CMS-Wave results plotted against SWAN results, including also the correction shown in Figure 4b.

5. Conclusions

The paper presents a comparison among three spectral wave models for wind-wave generation and propagation inside enclosed basins. The three chosen models are SWAN, STWAVE, and CMS-Wave, which are freely available and solve the spectral action balance equation. The three models are nowadays commonly used to develop wave statistics for the design of important coastal structures. In real applications, specific calibration is frequently not carried out, due to lack of sufficient wave information, and therefore also in this study the main default settings and parameters, that are those reasonably chosen by most designers, are used.

It was found that, for enclosed basins, the difference among the results obtained by uncalibrated models is larger than expected and not acceptable, in contrast to published results that are relative to open sea applications.

The comparisons were initially performed on an idealized case to focus on the effect of the differences among the wind input parameterizations. The differences in the investigated range of winds (10 m/s to 40 m/s) are significant. CMS-Wave gave inconsistent results especially for small fetches, due to an inherent threshold in the highest simulated frequency. SWAN predicted waves higher (up to 25% higher) than STWAVE. For SWAN, the ST6 Package was compared to the KOMEN one, and, as expected by the analysis of Christakos et al. [16], lower values of Hs were predicted.

An additional application on the Garda Lake (Italy) was carried out. This enclosed basin was selected as an example of a case where calibration is not possible due to the absence of combined information on wind and waves. The models were applied to two locations on the lake, where a recent project is underway, and differences in the wave height >20% were found, which are considered too large to be acceptable for design purposes. This study shows that a wave measurement campaign is necessary for this lake and in general for other similar enclosed basins.

The Full and Half plane modes in STWAVE and CMS-Wave were compared. For an enclosed basin such as the Garda Lake, the Full mode should be preferred since the lateral boundaries are not fully adsorbing. Although the wave heights computed in 7 points along the centre line of the Garda Lake are similar, the benefits of the Full mode are evident close to the shore.

A critical issue of these spectral models was found to be the selection of the frequency discretization, which requires a careful pre-analysis. This issue is emphasized when iterative calculations for different wind velocities are carried out since the frequency range is kept constant by the models but the ideal range may be rather different. A possible workaround is to set a considerably wide frequency range even if very time consuming.

Author Contributions: Conceptualization, L.M.; methodology, L.M. and C.F.; investigation, C.F and E.M.P.V.; writing—original draft preparation, C.F.; writing—review and editing, L.M. and C.F.; supervision, P.R. and L.M.; project administration, L.M. All authors have read and agreed to the published version of the manuscript.

Funding: This research was partially funded by the project "Development of a new Wave Energy Converter named Wave Attenuator", Bando Centro Giorgio Levi Cases a tema vincolato, Prot. 8 del 20 January 2021 Fasc. 2021-III/13.1 and by the Venice 2021 research grant funded by Provveditorato for the Public Works of Veneto, Trentino Alto Adige, and Friuli Venezia Giulia, provided through the concessionary of State Consorzio Venezia Nuova and coordinated by CORILA (Consorzio per il coordinamento delle ricerche inerenti al sistema lagunare di Venezia).

Conflicts of Interest: The authors declare no conflict of interest.

References

1. Lavidas, G.; Venugopal, V. Application of numerical wave models at European coastlines: A review. *Renew. Sustain. Energy Rev.* **2018**, *92*, 489–500. [CrossRef]
2. Umesh, P.A.; Swain, J. Inter-comparisons of SWAN hindcasts using boundary conditions from WAM and WWIII for northwest and northeast coasts of India. *Ocean. Eng.* **2018**, *156*, 523–549. [CrossRef]
3. Wamdi Group. The WAM model—A third generation ocean wave prediction model. *J. Phys. Oceanogr.* **1988**, *18*, 1775–1810. [CrossRef]
4. Tolman, H.L. User manual and system documentation of WAVEWATCH III TM version 3.14. *Tech. Note MMAB Contrib.* **2009**, *276*, 220.
5. Booij, N.; Holthuijsen, L.H.; Ris, R.C. The "SWAN" wave model for shallow water. In *Coastal Engineering Proceedings*; Elsevier: Orlando, FL, USA, 1996; Volume 1, pp. 668–676.
6. Booij, N.R.R.C.; Ris, R.C.; Holthuijsen, L.H. A third-generation wave model for coastal regions: 1. Model description and validation. *J. Geophys. Res. Ocean.* **1999**, *104*, 7649–7666. [CrossRef]
7. Smith, J.M. Modeling nearshore transformation with STWAVE. In *ERDC/CHL CHETN I-64*; U.S. Army Engineer Research and Development Center: Vicksburg, MS, USA, 2001.
8. DHI. *MIKE 21 Spectral Waves FM, User Guide*; DHI, Agern Allé: Hørsholm, Denmark, 2017; Volume 5, p. 2970.
9. Lin, L.; Demirbilek, Z.; Mase, H.; Zheng, J.; Yamada, F. *CMS-Wave: A Nearshore Spectral Wave Processes Model for Coastal Inlets and Navigation Projects*; Engineer Research and Development Center Vicksburg MS Coastal And Hydraulics Lab: Vicksburg, MS, USA, 2008.
10. Cavaleri, L.; Abdalla, S.; Benetazzo, A.; Bertotti, L.; Bidlot, J.R.; Breivik, Ø.; van der Westhuysen, A.J. Wave modelling in coastal and inner seas. *Prog. Oceanogr.* **2018**, *167*, 164–233. [CrossRef]
11. Rusu, E.; Goncalves, M.; Guedes Soares, C. Evaluation of the wave transformation in an open bay with two spectral models. *Ocean. Eng.* **2011**, *38*, 1763–1781. [CrossRef]
12. Fonseca, R.B.; Gonçalves, M.; Guedes Soares, C. Comparing the performance of spectral wave models for coastal areas. *J. Coast. Res.* **2017**, *33*, 331–346. [CrossRef]
13. Strauss, D.; Mirferendesk, H.; Tomlinson, R. Comparison of two wave models for Gold Coast, Australia. *J. Coast. Res.* **2007**, *50*, 312–316.
14. Ilia, A.; O'Donnell, J. An Assessment of Two Models of Wave Propagation in an Estuary Protected by Breakwaters. *J. Mar. Sci. Eng.* **2018**, *6*, 145. [CrossRef]
15. Moeini, M.H.; Etemad-Shahidi, A. Application of two numerical models for wave hindcasting in Lake Erie. *Appl. Ocean Res.* **2007**, *29*, 137–145. [CrossRef]
16. Christakos, K.; Björkqvist, J.V.; Tuomi, L.; Furevik, B.R.; Breivik, Ø. Modelling wave growth in narrow fetch geome-tries: The white-capping and wind input formulations. *Ocean Model.* **2021**, *157*, 101730. [CrossRef]
17. Aydoğan, B.; Ayat, B. Performance evaluation of SWAN ST6 physics forced by ERA5 wind fields for wave prediction in an enclosed basin. *Ocean Eng.* **2021**, *240*, 109936. [CrossRef]
18. Bellotti, G.; Franco, L.; Cecioni, C. Regional Downscaling of Copernicus ERA5 Wave Data for Coastal Engineering Activities and Operational Coastal Services. *Water* **2021**, *13*, 859. [CrossRef]
19. Martinelli, L.; Ruol, P.; Favaretto, C. Analysis of overflow and wave overtopping of the Scardovari lagoon levees. In Proceedings of the 31st International Ocean and Polar Engineering Conference, Rhodes, Greece, 20–25 June 2021.

20. Favaretto, C.; Volpato, M.; Martinelli, L.; Ruol, P. Numerical investigation on wind set-up and wind waves in front of Piazza San Marco, Venice (IT). In Proceedings of the 30th International Ocean and Polar Engineering Conference, Virtual Conference, 11–16 October 2020.
21. Nassar, K.; Masria, A.; Mahmod, W.E.; Negm, A.; Fath, H. Hydro-morphological modeling to characterize the adequacy of jetties and subsidiary alternatives in sedimentary stock rationalization within tidal inlets of marine lagoons. *Appl. Ocean. Res.* **2019**, *84*, 92–110. [CrossRef]
22. Bryant, M.A.; Jensen, R.E. Application of the nearshore wave model STWAVE to the North Atlantic coast comprehensive study. *J. Waterw. Port Coast. Ocean. Eng.* **2017**, *143*, 04017026. [CrossRef]
23. Lin, L.; Demirbilek, Z.; Thomas, R.C.; Rosati, J. Verification and validation of the coastal modeling system. In *Report 1: Summary Report*; US Army Corps of Engineers, Coastal Engineering Research Center: Vicksburg, MS, USA, 2011.
24. Sartini, L.; Mentaschi, L.; Besio, G. Evaluating third generation wave spectral models performances in coastal areas. An application to Eastern Liguria. In Proceedings of the OCEANS 2015—Genova, Genova, Italy, 18–21 May 2015; pp. 1–10.
25. Zundel, A.K. *Surface-Water Modeling System Reference Manual—Version 9.0*; Brigham Young University Environmental Modeling Research Laboratory: Provo, UT, USA, 2006.
26. Cavaleri, L.; Malanotte-Rizzoli, P. Wind wave prediction in shallow water: Theory and applications. *J. Geophys. Res.* **1981**, *86*, 10961–10973. [CrossRef]
27. Komen, J.G.; Hasselmann, S.; Hasselmann, K. On the existence of a fully developed wind-sea spectrum. *J. Phys. Oceanogr.* **1984**, *14*, 1271–1285. [CrossRef]
28. Janssen, P.A.E.M. Wave induced stress and the drag of air flow over sea waves. *J. Phys. Oceanogr.* **1989**, *19*, 745–754. [CrossRef]
29. Yan, L. *An Improved Wind Input Source Term for Third Generation Ocean Wave Modeling*; Scientific Report; Koninklijk Nederlands Meteorologisch Instituut (KNMI): De Bilt, The Netherlands, 1987.
30. Plant, W.J. A relationship between wind stress and wave slope. *J. Geophys. Res. Ocean* **1982**, *87*, 1961–1967. [CrossRef]
31. Rogers, W.E.; Babanin, A.V.; Wang, D.W. Observation-consistent input and whitecapping dissipation in a model for wind-generated surface waves: Description and simple calculations. *J. Atmos. Ocean Technol.* **2012**, *29*, 1329–1346. [CrossRef]
32. Wu, J. Wind-stress coefficients over sea surface from breeze to hurricane. *J. Geophys. Res.* **1982**, *87*, 9704–9706. [CrossRef]
33. Zijlema, M.; Van Vledder, G.P.; Holthuijsen, L.H. Bottom friction and wind drag for wave models. *Coast. Eng.* **2012**, *65*, 19–26. [CrossRef]
34. Hwang, P.A. A note on the ocean surface roughness spectrum. *J. Atmos. Ocean Technol.* **2011**, *28*, 436–443. [CrossRef]
35. Resio, D.T. Shallow-water waves. II: Data comparisons. *J. Waterw. Port Coast. Ocean Eng. ASCE* **1988**, *114*, 50–65. [CrossRef]
36. Lin, R.Q.; Lin, L. Wind input function. In Proceedings of the 8th International Workshop on Wave Hindcasting and Prediction, North Shore, HI, USA, 14–19 November 2004; pp. 14–19.
37. Phillips, O.M. On the generation of waves by turbulent wind. *J. Fluid Mech.* **1957**, *2*, 417–445. [CrossRef]
38. SWAN. *Scientific and Technical Documentation, SWAN Cycle III Version 41.11 AB.*; Delft University of Technology: Delft, The Netherlands, 2021; p. 152.
39. Battjes, J.A.; Janssen, J.P.F.M. Energy loss and set-up due to breaking of random waves. In Proceedings of the 16th International Conference on Coastal Engineering, Hamburg, Germany, 27 August–3 September 1978; pp. 569–587.
40. Madsen, O.S.; Poon, Y.K.; Graber, H.C. Spectral wave attenuation by bottom friction: Theory. In *Coastal Engineering Proceedings*; Coastal Engineering Reserach Council: Torremolinos, Spain, 1988; Volume 1, pp. 492–504.
41. Bretschneider, C.L.; Krock, H.J.; Nakazaki, E.; Casciano, F.M. Roughness of typical Hawaiian terrain for tsunami run-up calculations: A users manual. In *JKK Look Laboratory Report*; University of Hawaii: Honolulu, HI, USA, 1986; p. 42.
42. SWAN. *SWAN User Manual, SWAN Cycle III Version 41.11 AB.*; Delft University of Technology: Delft, The Netherlands, 2021; p. 146.
43. Ardhuin, F.; Rogers, E.; Babanin, A.V.; Filipot, J.F.; Magne, R.; Roland, A.; Van der Westhuysen, A.; Queffeulou, P.; Lefevre, J.M.; Aouf, L.; et al. Semiempirical dissipation source functions for ocean waves. Part I: Definition, calibration, and validation. *J. Phys. Oceanogr.* **2010**, *40*, 1917–1941. [CrossRef]
44. Sakai, S.; Kobayashi, N.; Koike, K. Wave breaking criterion with opposing current on sloping bottom: An extension of Goda's breaker index. *Annu. J. Coast. Eng.* **1989**, *36*, 56–59. (In Japanese)
45. Hurdle, D.P.; Stive, R.J.H. Revision of SPM 1984 wave hindcast model to avoid inconsistencies in engineering applications. *Coast. Eng.* **1989**, *12*, 339–351. [CrossRef]
46. Coastal Engineering Research Center (US). *Shore Protection Manual*; Department of the Army, Waterways Experiment Station, Corps of Engineers, Coastal Engineering Research Center: Vicksburg, MS, USA, 1984.
47. Nekouee, N.; Hamidi, S.A.; Etemadi, R. Sensitivity analysis of numerical wave predictions models, considering wind and geometry effects in rectangular lakes. *Ocean Eng.* **2015**, *104*, 549–557. [CrossRef]
48. US Army Corps of Engineers, Coastal Engineering Research Center. *Coastal Engineering Manual*, 5th ed.; US Army Corps of Engineers, Coastal Engineering Research Center: Vicksburg, MS, USA, 2003.
49. Massel, S.R. *Ocean Surface Waves: Their Physics and Prediction*; World Scientific: Singapore, 1996; Volume 11.
50. Nash, J.E.; Sutcliffe, J.V. River Flow forecasting through conceptual models-Part I: A discussion of principles. *J. Hydrol.* **1970**, *10*, 282–290. [CrossRef]

51. Willmott, C.J.; Ackleson, S.G.; Davis, R.E.; Feddema, J.J.; Klink, K.M.; LeGates, D.R.; O'Donnell, J.; Rowe, C.M. Statistics for the evaluation and comparison of models. *J. Geophys. Res. Space Phys.* **1985**, *90*, 8995. [CrossRef]
52. Lin, L.; Demirbilek, Z.; Thomas, R.C.; Rosati, J. *Verification and validation of the coastal modeling system*; In Report 2: CMS-Wave; US Army Corps of Engineers, Coastal Engineering Research Center: Vicksburg, MS, USA, 2011.
53. Hinegk, L.; Adami, L.; Zolezzi, G.; Tubino, M. Implications of water resources management on the long-term regime of Lake Garda (Italy). *J. Environ. Manag.* **2022**, *301*, 113893. [CrossRef]
54. Giovannini, L.; Laiti, L.; Serafin, S.; Zardi, D. The thermally driven diurnal wind system of the Adige Valley in the Italian Alps. *Q. J. R. Meteorol. Soc.* **2017**, *143*, 2389–2402. [CrossRef]
55. Giovannini, L.; Laiti, L.; Zardi, D.; de Franceschi, M. Climatological characteristics of the Ora del Garda wind in the Alps. *Int. J. Climatol.* **2015**, *35*, 4103–4115. [CrossRef]
56. De León, S.P.; Soares, C.G. Sensitivity of wave model predictions to wind fields in the Western Mediterranean sea. *Coast. Eng.* **2008**, *55*, 920–929. [CrossRef]
57. Bottema, M.; van Vledder, G. Effective fetch and non-linear four-wave interactions during wave growth in slanting fetch conditions. *Coast. Eng.* **2008**, *55*, 261–275. [CrossRef]